SSRG International Journal of Electrical and Electronics Engineering
ISSN: 2348-8379/ https://doi.org/10.14445/23488379/IJEEE-V11I6P134

Volume 11 Issue 6, 338-350, June 2024

Original Article

Performance Evaluation of MIMO-OSTBC System at mm-Wave Frequency

Priyadarshini K. Desai[1], Keerti Kulkarni[2]

[1,2]*Department of Electronics & Communication Engineering, B.N.M. Institute of Technology, Karnataka, India.*

[1]*Corresponding Author : priyadarshini.p.r@gmail.com*

Received: 16 April 2024 Revised: 18 May 2024 Accepted: 16 June 2024 Published: 29 June 2024

Abstract *- The present wireless communication technology uses MIMO-Orthogonal Space-Time Block Code to improve wireless system performance (MIMO-OSTBC). It is very well known that in any MIMO system, closely placed antennas result in mutual coupling. The presence of mutual coupling degrades MIMO-OSTBC transmission performance. Hence, there is a necessity to design a multiple-antenna system, offering minimum mutual interaction that will result in performance enhancement of the MIMO-OSTBC system. This work mainly includes a 2x2 MIMO antenna system design for 24GHz frequency operation. The radiating elements are spaced at a distance of λ/4 from each other in the proposed design of a 2x2 MIMO system. The evaluation of the 2x2 MIMO system, with and without decoupling structure, is carried out through performance evaluation metrics such as ECC and TARC. The isolation of -33dB is achieved by introducing a Defected Ground Structure (DGS) and -22dB without decoupling structure. The CST tool is used to design and simulate a 2x2 multiple antenna. The simulated 2x2 multiple antenna is fabricated. The observed and simulated results accord with each other rather well. Next, an orthogonal STBC performance analysis is performed on 2x2 multi-antenna systems with and without isolation structures. The obtained results show that the reduction of mutual interaction (due to the introduction of Defective Ground Structure) improves the MIMO-STBC system's overall performance (measured through Bit Error Rate).*

Keywords *- Bit Error Rate, Defected Ground Structure, Microstrip Rectangular Patch Antenna (MRPA), Multiple antenna system, mm-wave, OSTBC.*

1. Introduction

The state of wireless communication technology has evolved significantly to meet consumer needs for fast data rates, minimal latency, and continuous connectivity. Any technological development is primarily the product of smart hardware design engineering and the application of better algorithms. The present state of 4G-LTE indicates that all of its available spectrum is occupied, making it unable to satisfy consumer demand. Thus, moving the communication band to a higher frequency range is necessary, and the following high-frequency spectrum contains the mm-wave band. When a signal is transmitted in the mm-wave band, it experiences significant attenuation and cannot satisfy the need for long-range communication. A multiple-input, multiple-output system, also termed as a multiple antenna system, is employed to counter this loss of propagation. The introduction of multi-antenna system technology greatly increases the system output.

In a multiple-antenna system, the transmitter and receiver incorporate more than one antenna. Recent years have seen much interest in multiple antenna designs, which constitute the foundation of all modern communication systems.

The performance of a multi antenna system depends on the spacing gap between the radiating elements. When the radiating elements show little interaction with their surrounding elements, there is always an enhancement in MIMO system performance. In any fading channel, better diversity is attained using a variety of coding methods along with multiple antenna systems. Orthogonal space-time block code is one such channel coding method.

Basically, space-time block coding sends numerous copies of data over the available number of antennas and makes use of various versions of the data that are received to increase data transfer reliability. Therefore, the construction of closely spaced radiating elements with less coupling and better channel coding techniques is the primary requirement to achieve better system performance.

The work carried out is primarily split into two sections. The first part explains the design of an MRPA with a 24GHz resonance and the transformation of the same into a 2x2 multiple antenna system. The efficacy of the multiple antennas is assessed both with and without a defective ground structure. The envelope-correlation coefficient, diversity gain, mean-

effective gain, channel capacity loss, and total-active reflection coefficient are the fundamental evaluation performance metrics used for the assessment of the designed multiple-antenna. The single microstrip rectangular patch antenna and 2x2 multi-antenna are designed and simulated using CST microwave studio.

The further part of the work includes performance evaluation of OSTBC with the designed 2x2 multiple antenna system, for transmission of signal over the Multiple-Input, Multiple-Output channel. The performance analysis of 2x2 MIMO is carried out using MATLAB. A literature survey related to various channel coding techniques and various decoupling methods used in the Multiple-Input and multiple-output is discussed in Section 2. Section 3 discusses the methodology of the work.

In Section 4, the design and analysis of multiple antenna systems are discussed. Initially, the copper-based MRPA is constructed on the dielectric substrate Roger 5880, which has a 2.2 relative permittivity and a thickness of 0.508mm. As a result of its low loss at millimetre frequency, the Roger 5880 is employed. The dimension of the ground is taken to be 15 x 15 x 0.017 mm^3.

Later, a 2x2 multi-antenna is derived from the designed single rectangular microstrip patch antenna. The performance metrics for a 2x2 multi-antenna device with and without a decoupling structure are assessed. Section 5 analyses the OSTBC coding technique's effectiveness with a designed 2x2 multi-antenna system. The conclusion of the work is detailed in Section 6.

2. Literature Review

A better data rate, with lower BER in any wireless system, can be achieved with an increase in transmission power and channel bandwidth. Therefore, large transmitted power is needed to overcome severely fading channel circumstances [1]. As stated in Shannon's limit theorem, a communication-related mathematical theory, channel capacity depends on bandwidth and signal-to-noise ratio. According to this theory, data is consistently transmitted when the capacity of the channel is greater than the data rate. Information cannot be consistently transmitted if the capacity is less than the data rate, as stated in [3].

Any increase in SNR necessitates an equivalent increase in transmitted power, but the value of transmitted power is constrained by intersystem interference. When a signal is sent over a wireless network, various components in the medium can reflect, scatter, or diffract the signal, which is termed multipath propagation. Multipath propagation is based on the fact that when a signal travels over a wireless channel, it will arrive at the recipient at different times from different pathways in addition to the Line of Sight signal (LOS).

A diversity technique termed a multipath forward error correction technique is introduced in [4]. The work shows that BCH and RS code performance can be enhanced by incorporating multipath forward error correction techniques without increasing the number of redundancies.

Every antenna separated from the others in space by a certain distance suggests (received diversity) to combat the multipath impact at the receiver [5]. The demand from users for greater data rates in wireless communication systems is increasing in a band-limited echo system, which explains why numerous antennas are required.

In [6] a study of multiple-transmit and receive antennas for single-user communication over fading-free AGWN channels is made. The work shows that the implementation of a multiple-antenna system greatly increases the data rate on fading channels if channel parameters are estimated at the receiver and path gain between antenna pairs is independent.

The fundamental goal of multiple antenna is to increase data rate (bits/sec) and quality (BER). To increase spatial diversity and bring significant capacity gains, Space-Time Block Codes (STBCs) in combination with multiple antenna are extremely helpful, as discussed in [7].

Work in [8] concentrated on Orthogonal Space-Time Block Codes (OSTBC) as they give the system spatial variety, which in turn reduces the impact of multipath fading on multiple antenna communications systems and greatly enhances link quality. Since code accomplishes better diversity, coding gain, and throughput.

Alamouti's work in [9] proposed an appealing method in 1998 for communications in a non-dispersive Rayleigh fading channel using two transmitters in conjugation with any number of receivers.

Alamouti's work was popularized in 1999 by Tarokh and coworkers et al. in [9] to any number of receivers. With the help of a multipath environment that can high diversity gain is achieved requiring no additional bandwidth, this strategy produced the STBC code, which exhibits remarkable encoding and decoding ease while achieving excellent performance.

In order to take advantage of the multiple antenna in a fading channel and reduce transmission errors at the receiver, space-time coding is incorporated to create a correlation between transmitted signals from different radiating antenna elements at particular times is discussed in [10].

It has been demonstrated that space-time block codes are an effective method for delivering high data-rate wireless communication [11]. The Alamouti scheme, which uses 2 transmit antennas, is the only configuration for STBCs that

can reach a full code rate discussed in [9]. The benefits of combining space-time block coding with numerous transmit and/or receive antennas have been properly examined in [9] and are now widely acknowledged.

In particular, it has been demonstrated that the OSTBC of [9, 12] offer complete diversity with complexity only in linear decoding. In [9], work states that system that has more than two transmit antennas, full-rate OSTBCs do not exist. However, for these codes to function properly, a precise understanding of the channels between the broadcast and receive antennas is required. Tarokh, Jafarkhani, and Calderbank created a theoretical foundation for generalized orthogonal designs based on the notion of classical orthogonal designs for transmission employing multiple transmit antennas.

Later, the idea was used to build Space-Time-Block-Codes (STBC) for a large number of transmit antenna elements using generalized orthogonal designs. Research on channel estimation for multiple-input, multiple-output systems has been driven by the significance of channel information to space-time coding carried out in [13–17].

In [18] diversity order of STBCs is discussed. A decoupled maximum-likelihood decoding algorithm and full diversity order are two elements of STBC that, according to research, prevent the receiver's maximum likelihood decoding from becoming exponentially complex. The underlying orthogonal and decoupled structure of the STBCs results in a reduction in complexity in terms of the number of broadcast information symbols that can be processed within the receiver's allowed decoding time.

The incorporation of the Butler matrix in 4*4 multiple antenna systems is discussed in [19]. The proposed method increases multiple antenna system capacity using the concept of angular domain processing. The authors found higher efficiency compared to multiple antenna systems. The efficacy of Open-Loop Active Propagation Control (OLAPC) on multiple antenna and SISO channel capacities was estimated in [20]. The authors discovered that OLAPC could be used to increase the smaller channel capacity successfully.

The use of multiple antenna to enhance the capacity of communication channels is discussed in [21]. The work concluded that the capacity in the channel can be enhanced by incorporating a multi-antenna system with a beam pattern antenna with a capacity that is higher than a traditional antenna like a dipole antenna. The antenna uses factors such as polarization, array configuration, and field pattern to improve the channel capacity.

The contributions of research work are devoted to analyzing and assessing the impact of the coding method (represented by STBC code) to enhance the capacity of the channel over multiple-antenna systems with various numbers of antennas. Also shows how using various types of carrier modulation schemes over Rayleigh fading channels can improve the bit-error rate of a multiple antenna system's performances. The single-element antenna design for a multiple-antenna system is equally as essential as channel coding techniques.

The analysis of a typical patch antenna with a change in dimension and shape to increase bandwidth for Ultra-wideband applications is discussed in [22]. The intended radiating element is changed to a 2x2 multiple antenna, and a meta-surface made of SRR acts as the decoupling structure. The work reveals a -43 dB transmission coefficient. The envelope correlation coefficient and diversity increase are 0.07 and 10dB, respectively. The results show that the use of metamaterial structure resulted in reduced mutual coupling among radiating elements at UWB frequency.

As a decoupling structure, a special flower-shaped metamaterial absorber has been developed [23]. The multiple antenna for the 5.5 GHz WiMAX spectrum is designed. A line between two radiating elements is meant to be formed by a metamaterial absorber with a four-element array. The separation level obtained is -33dB. The performance measures for multiple antennas that were evaluated were ECC, DG, and TARC. However, the radiation efficiency was 68.03% despite the observed ECC and DG values of 0.004 and 10 dB, respectively. The radiation effectiveness was decreased due to the presence of the partial ground construction.

A meta-surface is incorporated in an antenna array as an isolating structure method to reduce mutual interaction in multiple-antenna systems [24]. A meta-surface made of SRR and tuned to 5.8GHz suspends two-element multiple antenna arrangements from it. Isolation at the ideal frequency band is -27dB with 0.08 ECC.

In [25], the isolation in multiple-antenna systems is enhanced by utilizing hybrid electric and magnetic coupling structures. The multiple antenna setup operates between 2.3 and 2.8GHz. The device that freed the emitting element from its coupling was a split ring resonator.

A decoupling factor of -30 dB was accomplished using a split ring construction. The envelope correlation coefficient obtained is less than 0.005, which is incredibly low between 2.3GHz and 2.9GHz. The variation in channel capacity loss from 1.28 to 16.55 bps/Hz is observed for the multiple-antenna system designed to radiate in the sub-6GHz frequency band.

A quad-band antenna with better isolation multiple antenna is employed in the construction of broadband SCS for broadcasting and communications purposes is discussed in [26].

Self-complementary structure loaded dual PIFA antenna resulted in the quad-band. The designed dual PIFA is perfect for WLAN at 2.4GHz and 5.15GHz, L-band and UHF, with acceptable impedance matching. The transmitters were first positioned to be aligned orthogonally.

The antenna was excited through a connecting line used close to the input point, acting in a manner similar to a 2-GHz band stop filter. On the lower side of the antenna, a connecting plane is incorporated as a final step. All three methods employed made the antenna operate at three different frequencies. The antenna elements' obtained isolation is -30 dB.

The compact multiple-antenna construction and investigation for WLAN and WiMAX are discussed in [27]. The author used the orthogonal arrangement of the antenna elements and along with this antenna element arrangement, a Y-shaped non-radiating element was placed in between the radiating antenna elements.

The antenna array system with the dimensions of 20mm X 20mm in designed and investigated in [28]. The transmission coefficient between elements obtained is -43 dB and the Envelope-Correlation-Coefficient obtained is approximately 0.004 at 80% radiation effectiveness. The major benefits of the MIMO system are a 10x time increase in capacity and a concurrent 100x time increase in radiated energy efficiency, according to a survey [28]. It is claimed that the use of more compact antennas will result in a substantial improvement in energy efficiency.

The phase shift technique is used to act as a distinctive isolating structure [29]. The work proposes a novel antenna design that basically consists of a λ/2 strip line along with a shorting pin.

The mutual interaction among the adjacent patch antennas is minimized due to the presence of an additional signal line. At 3.16GHz, the operating frequency of the mutual interaction among the patch antenna has improved by 7-8dB. The characteristic modes are used in antenna design to analyze the behavior of a flawed ground layer construction [30].

The analysis is done using a methodical procedure to see if the isolation factor can be improved. For the case study, separate monopole and PIFA elements were used to build two 4-radiating elements and one 2-radiating element multiple antenna system. The work concludes that the addition of DGS could improve isolation by 11 dB.

To increase isolation, two additional kinds of feed lines are also used, one designed using SIW cavity and the other on plasmon surface polarization [31]. The high-pass and low-pass input networks of the SIW and SSP enable broadband decoupling character.

3. Methodology

Figure 1 provides the systematic flow chart as to how the proposed work is to evaluate MIMO-OSTBC performance.

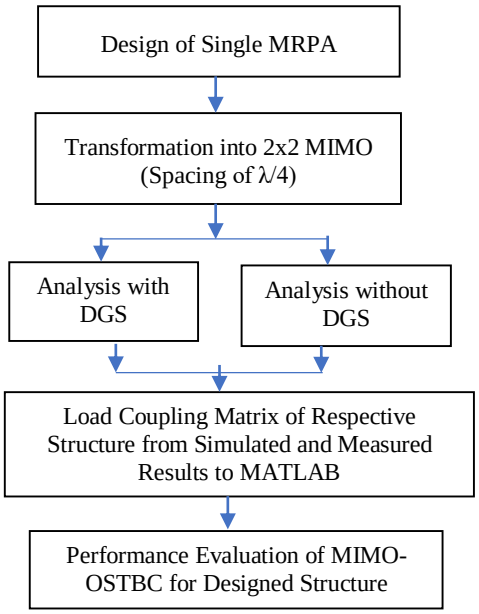

Fig. 1 Methodology of the proposed work

The design of MRPA operating at 24GHz is carried out. The substrate Roger 5880 with dimensions is 15 x 15 x 0.508) mm^3. Further, the single MRPA is converted to a 2x2 MIMO system. In the design process of the 2x2 MIMO antenna system, the dielectric substrate dimension is retrieved to be the same as that of the single MRPA. This design criterion, where the substrate dimension is the same for single MRPA and 2x2 MIMO, is what makes the overall system to be compact. Fabrication of the designed 2x2 MIMO antenna system incorporated with decoupling structure, i.e. DGS, is done. Further, the performance of the 2x2 MIMO antenna system with and without DGS structure is assessed. The coupling matrix of 2x2 MIMO is taken, and through the MATLAB tool, the OSTBC system performance is analyzed with the designed 2x2 MIMO (both with and without DGS). In the analysis of OSTBC, four cases are considered, namely, no coupling, which is an idle case, followed by the proposed 2-port multiple antenna with and without DGS is simulated, fabricated and also measured.

4. Proposed Multiple Antenna System

This study, basically a 2x2 MIMO antenna system, is designed and simulated. A rectangular shape slot is cut in the ground metal plane to improve the isolation between the elements. The design of a single MRPA resonant at 24 GHz is discussed in section 4.1. The performance measures used in the evaluation of multiple-antenna systems are discussed in section 4.2. The design and study of 2x2 MIMO antenna system at 24GHz without defective ground structure is disucussed in section 4.3. The performance evaluation of 2x2

MIMO without DGS structure is analyzed in section 4.4. The analysis and design microstrip patch antenna measuring 2x2 with DGS is analyzed in section 4.5. The performance evaluation of 2x2 MIMO antenna system with defected ground is discussed in section 4.6.

4.1. Microstrip Rectangular Patch Antenna (MRPA) Design and Analysis

In a microstrip rectangular patch antenna, the dielectric substrate is sandwiched between the two metallic pieces. The metallic layer below the substrate is termed the ground layer, and the above layer is a radiating patch. In most cases, the substrate has a dimension of λ/2 x λ/2. Usually, dielectric material with minimal substrate loss is preferred when operating at higher frequencies. The Rogger 5880 substrate is selected due to its dielectric constant of 2.2, the height of 0.5mm, and the required frequency of operation is 24GHz. To determine the breadth and length of the patch antenna, the Equations (1) through (5) are used.

$$W_{patch}=\frac{c}{2f_0\sqrt{\frac{\varepsilon_r+1}{2}}} \quad (1)$$

$$L_{patch} = L_{eff} - 2\Delta L \quad (2)$$

$$\Delta L = 0.412t_s \frac{(\varepsilon_{eff}+0.3)(\frac{W}{t_s}+0.264)}{(\varepsilon_{eff}-0.258)(\frac{W}{t_s}+0.8)} \quad (3)$$

$$L_{eff} = \frac{C}{2f_0\sqrt{\varepsilon_{eff}}} \quad (4)$$

$$\varepsilon_{eff} = \frac{\varepsilon_r+1}{2} + \frac{\varepsilon_r-1}{2}[1+12\frac{t_s}{W}]^{-1/2} \quad (5)$$

MRPA has the following measurements: patch width $=W_{patch}$ = 4.23mm and patch length=L_{patch} = 4.11mm. For the antenna to operate at a frequency of 24GHz, it is intended to have the ideal length and width, which needs to be varied. Since a microstrip line is used as the input line, proper impedance matching is established between MRPA and transmission line, i.e. microstrip line. The microstrip line's characteristic impedance is basically a function of the line's height, breadth, and permittivity, as shown in Equation (6).

$$Z_c = \frac{120\pi}{\sqrt{\varepsilon_{eff}}\left[\frac{W_f}{t_s}+1.393+0.667\ln\left(\frac{W_f}{t_s}+1.44\right)\right]} \quad (6)$$

Where, t_s is the substrate's height, W_f is the line's breadth, and ε_{eff} is the substrate's effective permittivity. The feed width is parametrically changed to obtain sufficient impedance matching. A 0.5mm width of feedline offered improved impedance matching. Figure 2 depicts the designed MRPA, and S_{11} is indicated in Figure 3. The actual/real dimensions of the designed MRPA are displayed in Table 1. Figure 4 depicts the intended antenna's far-field pattern.

Table 1. Dimensions of MRPA

MRPA Layer	Parameter	Size
Metal Ground	Gnd_Length (L_G)	15mm
	Gnd_Width (W_G)	15mm
	Thickness (t_G)	0.017mm
Dielectric Material	Dielectric_Width (Ws)	15mm
	Dielectric _Length (Ls)	15mm
	Dielectric _Height (ts)	0.5mm
Rectangular Patch	Patch_Width (Wpatch)	4.74mm
	Patch_Length(Lpatch)	3.84mm

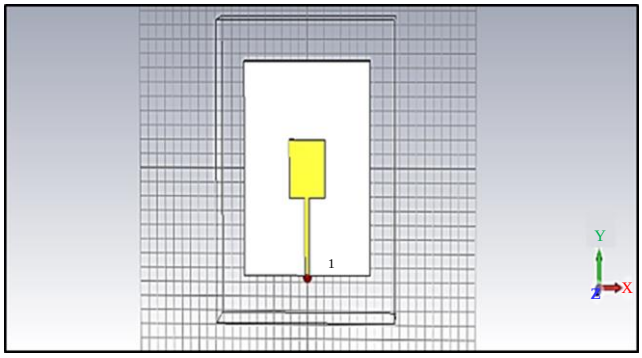

Fig. 2 Proposed MRPA

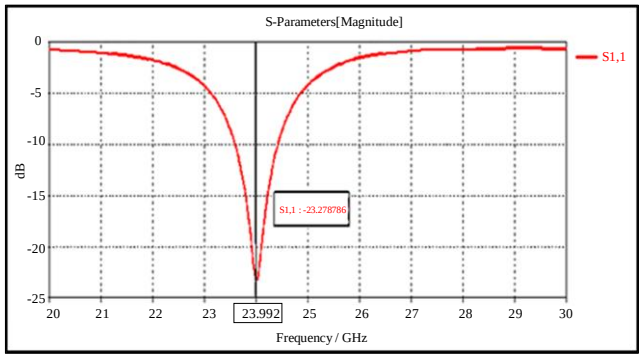

Fig. 3 Reflection coefficient plot of designed MRPA

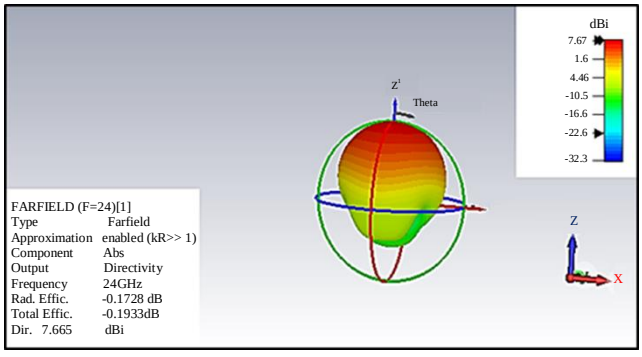

Fig. 4 The 3D far-field radiation pattern of MRPA

The reflection coefficient is -23 dB at 24GHz, indicating that the designed antenna resonates better at 24GHz and offers a directivity of 7.67dB.

4.2. Performance Metrics for Evaluation of Multiple-Antenna Systems

Numerous metrics are reported in the literature to assess the performance of a multiple antenna system; in this work, the Envelope-correlation-coefficient, Diversity -gain, Mean-effective-gain, Channel-capacity loss, and Total-active-reflection-coefficient metrics are used. The ECC assesses the correlation among the radiating elements. The correlation is assessed through both parameters, namely field pattern and S-parameters. Equation (7) is used to evaluate ECC using s-parameters, where i and j are antenna and N indicates the total number of antennas analyzed. The value of ECC must be less than 0.005 when assessed through S-parameters and smaller than 0.5 when assessed through the far-field pattern.

$$\rho_e = \frac{\left|\sum_{n=1}^{N} S_{i,n}^{*} S_{n,j}\right|^2}{\prod_{k=(i,j)} 1 - \sum_{n=1}^{N} S_{i,n}^{*} S_{n,k}} \tag{7}$$

To maintain the power standards, the Mean-Effective -Gain (MEG) of any two antennas in a MIMO-Antenna System must be -3dB. The incident average power to antenna average received power ratio is known as MEG. The power differential over a channel or propagation medium is assessed or evaluated by a MIMO-antenna system's mean effective gain. MEG is one of the vital metrics that determine how better a MIMO-antenna system works. The MEG computation is carried out using Equation (8).

$$MEG = \int_0^{2\pi}\int_0^{\pi}\left[\frac{XPR}{1+XPR} G_\theta(\theta,\varphi) P_\theta(\theta,\varphi) + \frac{XPR}{1+XPR} G_\theta(\theta,\varphi) P_\theta(\theta,\varphi)\right] sin\theta \, d\theta \, d\varphi \tag{8}$$

The antenna's power gain patterns are G_θ and G_ϕ. For a uniform propagation setting outside, XPR=0.

Diversity Gain measures how well MIMO-Antenna Systems work compared to Single Input Single Output (SISO). It is usually computed using relation (9). The highest diversity gains when using maximum-ratio combining is 10 at the 1% level of probability, and ep is the diversity gain reduction factor brought on by signal correlation among the two antennas. (e is the envelope correlation coefficient).

$$DG = 10 \times e_p = \sqrt{(1 - |0.99 e \rho_{ij}|)^2} \tag{9}$$

To characterize the frequency bandwidth and radiation performance of multiple antenna systems under the different natures of multiple antennas, TARC is a crucial metric. Even though the input signal phase varies for all input ports, it emphasizes the significance of impedance bandwidth and non-varying resonance frequency. After taking into account the TARC formulation provided in, a generalized equation of TARC has been developed for multiple-port antennas combining all scattering parameters when the antenna is linearly polarised (10).

$$TARC = \frac{\sqrt{\sum_{i=1}^{N}\left|S_{i1} + \sum_{m=2}^{N} S_{im} e^{j\theta_{m-1}}\right|^2}}{\sqrt{N}} \tag{10}$$

The crucial diversity performance evaluation criteria for many antennas include CCL. The CCL aids in indicating the highest achievable rate of message transmission up to which signal can be continuously transferred over the communication channel with a loss of less than 0.4 bits/s/Hz over the operating frequency range. It is obtained using Equation (11):

$$C_{loss} = -\log_2 det(\alpha^R) \tag{11}$$

where $\alpha^R = \begin{bmatrix} \alpha_{11} & \alpha_{12} & \alpha_{13} \\ \alpha_{21} & \alpha_{22} & \alpha_{23} \\ \alpha_{31} & \alpha_{32} & \alpha_{33} \end{bmatrix}$

Where $\alpha_{ii} = 1 - \sum_{j=1}^{N}\left|S_{ij}\right|^2$ and $\alpha_{ij} = -\left(S_{ii}^{*} S_{ij} + S_{ji}^{*} S_{ij}\right)$

4.3. Design and Study of 2x2 MIMO Antenna System at 24GHz without Defective Ground Structure

The MRPA designed at 24GHz frequency is converted into a 2x2 MIMO antenna system. The MRPA are spaced 3.0 mm which is equal to quarter wavelength distance. Figure 5 displays a setup with 2x2 multiple antennas.

The 2x2 system's reflection coefficient S_{11}, S_{22} and transmission coefficient S_{12}, S_{21} is depicted in Figure 6, demonstrating that both the antennas resonate at 24GHz and that the antennas also exhibit mutual coupling at that frequency.

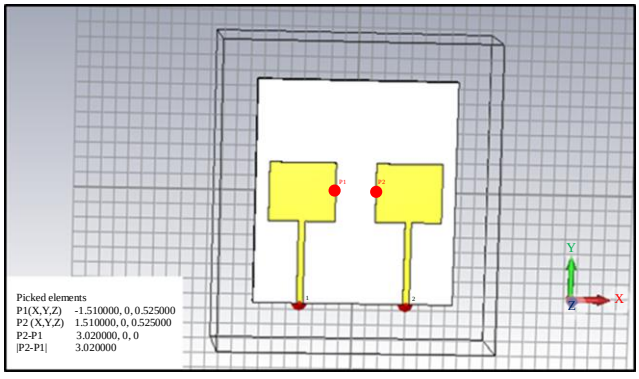

Fig. 5 2x2 Multiple antenna with λ/4 spacing

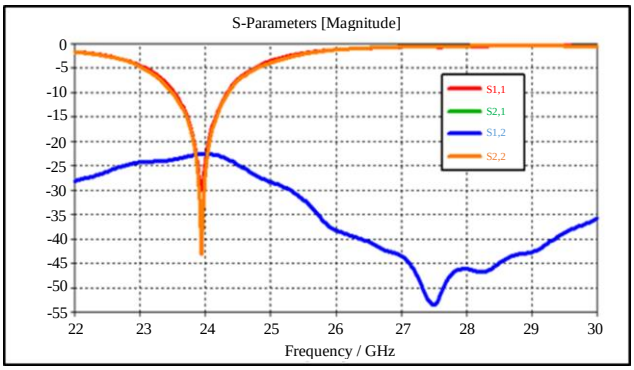

Fig. 6 The S_{11}, S_{22} and S_{12}, S_{21} of 2x2 multiple antenna system

The impedance matching of the microstrip transmission line, i.e., feed line and the MRPA, is better as the values of the S_{11} and S_{22} (reflection coefficient) of antennas 1 and 2 at 24GHz are -43dB. S_{12} and S_{21}, the transmission coefficients, are -23dB, indicating a lower level of isolation among the radiating elements. The reason for this interaction is the surface current distribution, and it can be noted that when either of the ports is excited, the mutual interaction takes place, which can be seen in Figure 7. The designed antenna's radiation efficacy is 96% and transmission effectiveness is 94%, respectively, for the 2x2 MIMO shown in Figure 8. The pattern generated by radiating MRPA also exhibits diversity in term angle orientation.

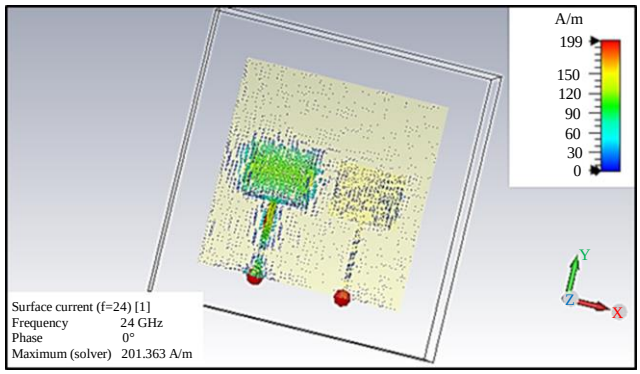

(a)

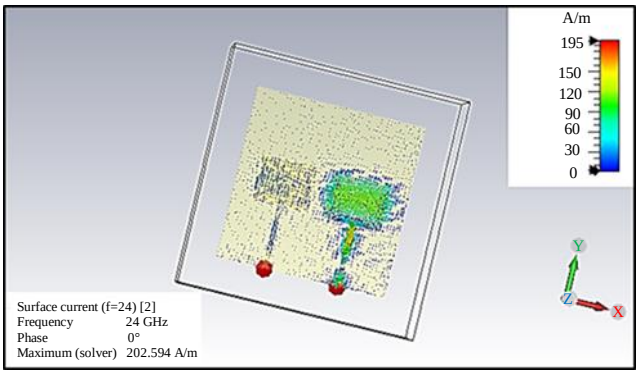

(b)

Fig. 7 Surface current antenna-1(a), and antenna-2 (b).

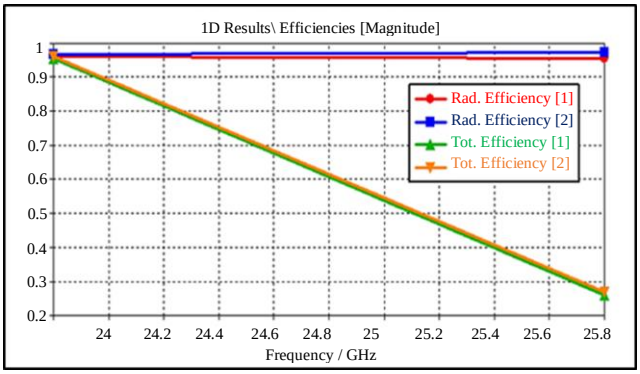

Fig. 8 Radiation and transmission efficiency of 2x2 antenna

Antenna 1's primary lobe's E-filed pattern is -18 degrees, while antenna 2's is +17 degrees. The antenna displays a variety of patterns, and when the pattern overlap (3dB) is greater than 90^0, the efficacy of multiple antenna systems suffers. Figure 9 shows the E-Field of antennas 1 and 2, which have a half power angular of $93^{0,}$ which indicates that the antennas exhibit a wider radiation beam.

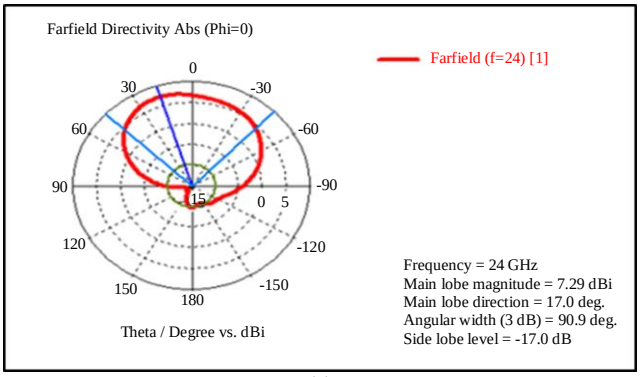

(a)

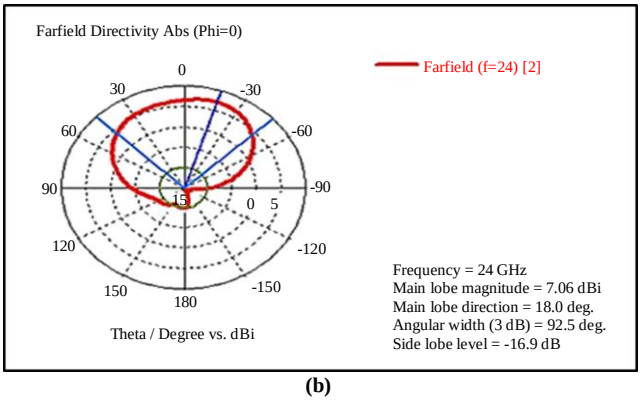

(b)

Fig. 9 E-field pattern of 2x2 MIMO antenna system (a) f=24 [1], and (b) f=24 [2].

4.4. Performance Evaluation of 2x2 MIMO without DGS Structure

The ECC assessed using both far-field patterns is around 0.00039, and through scattering parameters is around

$4.395x10^{-6,}$ which is indicated by Figures 10 (a) and (b). The DG for the 2x2 system is 9.99dB, and the MEG is -3.103dB, as indicated in Figures 11 (a) and (b).

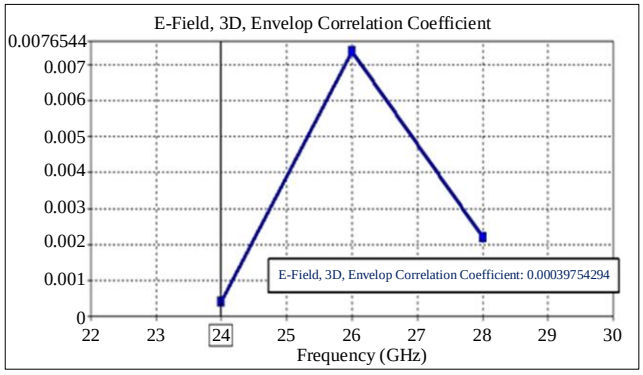

(a)

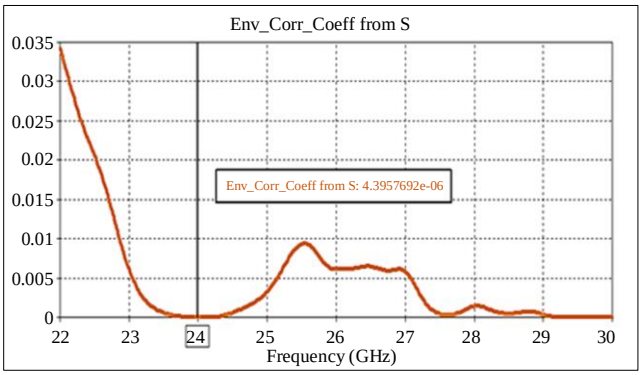

(b)

Fig. 10 Envelope correlation coefficient through (a) Far-field pattern, and (b) Scattering-parameter.

The channel capacity loss of the designed 2x2 MIMO is found to be $2.8x10^{-5}$ at 24GHz, as shown in Figure 12(a), and TARC illustrates the variation over the working frequency range, which is not less than 0dB in the required frequency range as shown Figure 12(b). TARC value at 24GHz is not below 0dB i.e. does not follow the S-parameters. The TARC values do not meet with the values reported in the literature, but the ECC, DG, and MEG values obtained do.

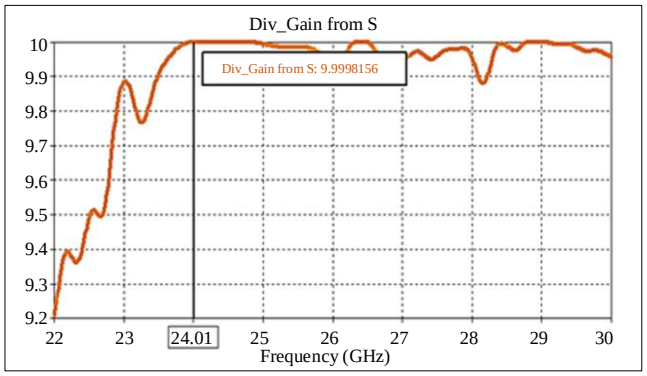

(a)

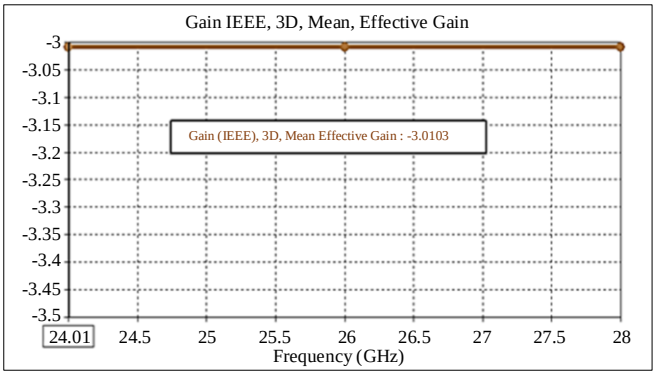

(b)

Fig. 11 2x2 MIMO (a) Diversity gain, and (b) MEG.

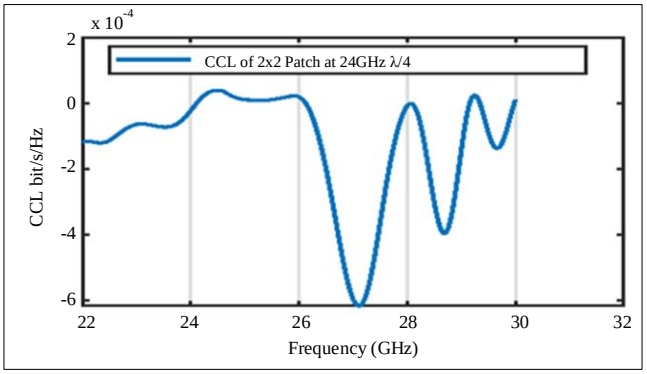

(a)

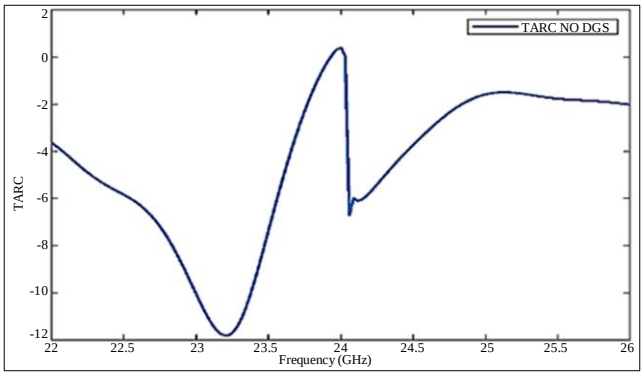

(b)

Fig. 12 2x2 multiple antenna system (a) CCL, and (b) TARC.

4.5. Analysis and Design Microstrip Patch Antenna Measuring 2x2 with DGS

A 2x2 multiple-antenna is introduced with defective ground. The ground metal has been introduced with a rectangular slot having a dimension of 2mm x 10mm. Figure 13 (a) shows the top view of the designed 2x2 microstrip patch antenna, while Figure 13 (b) depicts the lower view.

The discontinuity in the field interaction of the radiating elements, as well as the discontinuity in surface waves occurs due to rectangular slot introduction in the ground metal. The Scattering-parameter diagram in Figure 14 makes this

obvious. The S11 is -25dB, -20dB without and with DGS. During the simulations, it is observed that the interaction between the S11, S22 and S12, S21 does not exist in the required frequency band. Reduced contact among the two antenna elements is mainly due to the reduction in surface current which is very well depicted in Figure 15.

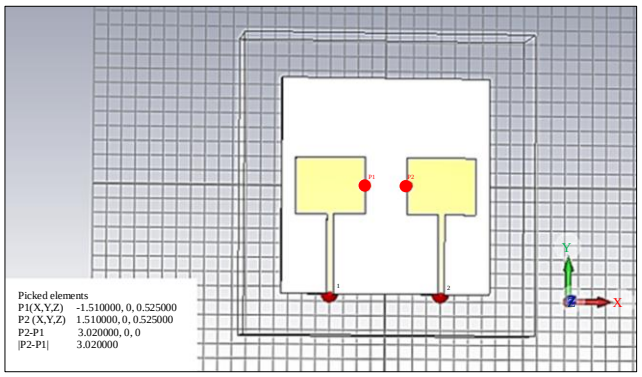

(a)

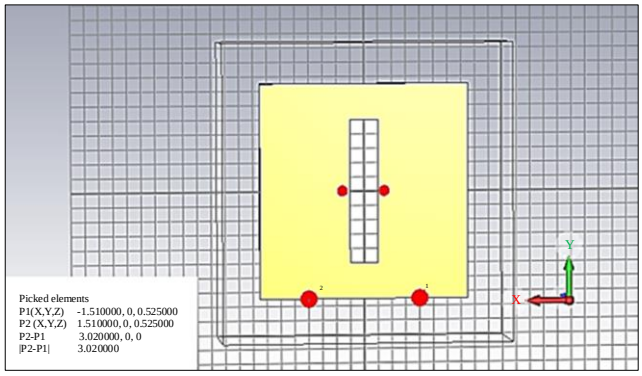

(b)

Fig. 13 Structure of 2x2 MIMO antenna with DGS (a) Top, and (b) Bottom.

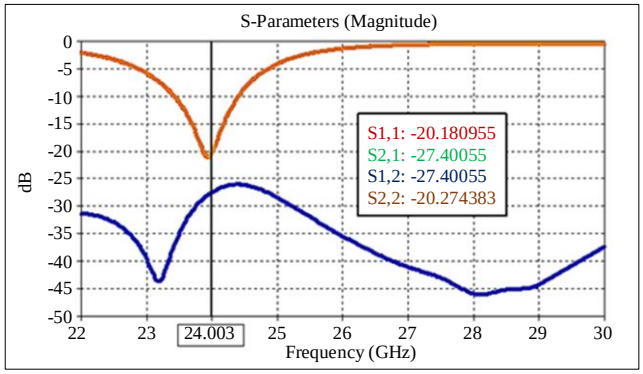

Fig. 14 S-parameter of 2x2 MIMO with DGS

The main lobe of antenna 1 is along +2 degree with an HPBW-3dB angular width of 60.5^0, and antenna 2 main- lobe is directed -20^0 with 3dB angular width of 60.4^0. The beam formed is narrower by 30^0 with the introduction of DGS. The E field pattern exhibits a pattern diversity of 20, as depicted in Figure 16.

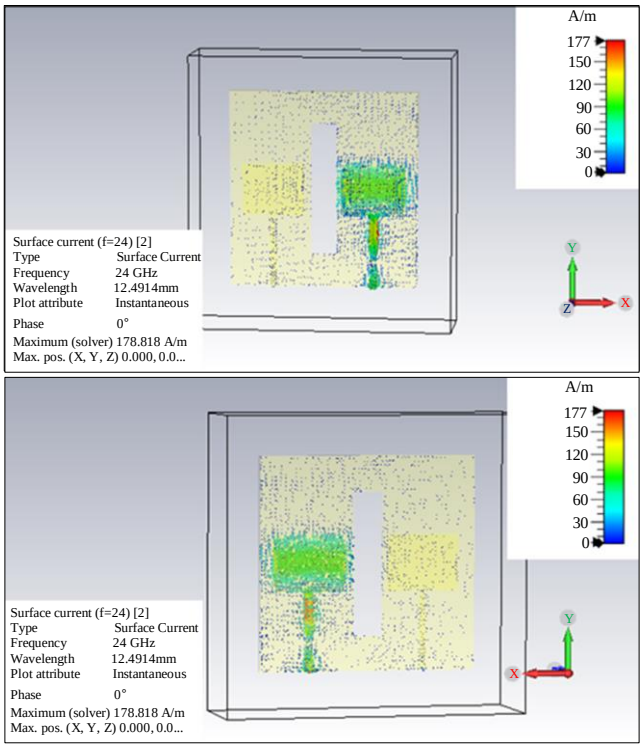

Fig. 15 Distribution of surface current for 2x2 MIMO with DGS

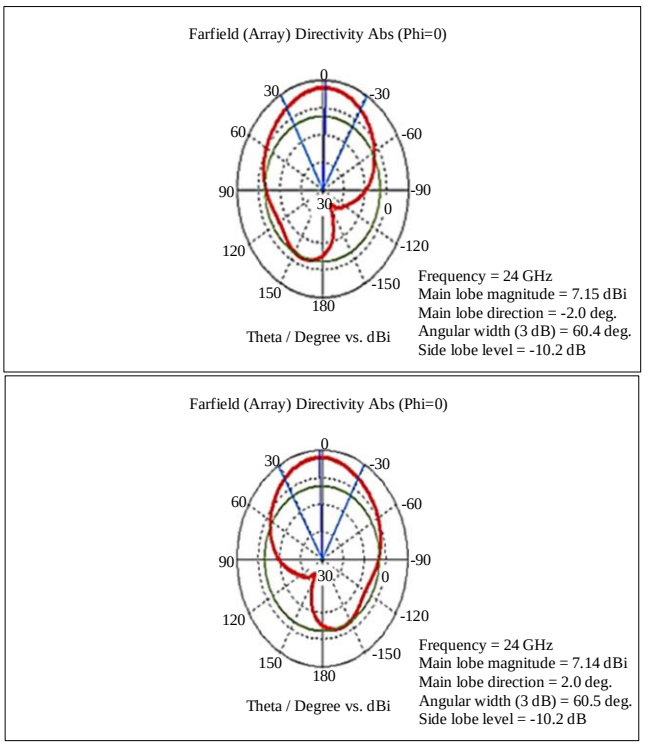

Fig. 16 E- field pattern of 2x2 antenna

4.6. Performance Evaluation of 2x2 MIMO Antenna System with Defected Ground

The ECC assessed through radiation pattern and scattering parameters is $4.14x10^{-6}$ and $9.0495x10^{-7,}$ as shown

in Figures 17 (a) and (b). The DG and the MEG for the 2x2 system are 9.99995dB and -3.103, as indicated in Figures 18 (a) and (b).

The 2x2 MIMO antenna system with DGS offers CCL of $6.043x10^{-6,}$ as indicated by Figure 19, and TARC is lower than 0dB and follows S-parameters in the required frequency range. Figure 19(b) depicts the plots of TARC for the 2x2 multiple-antenna system separated by λ /4 distance.

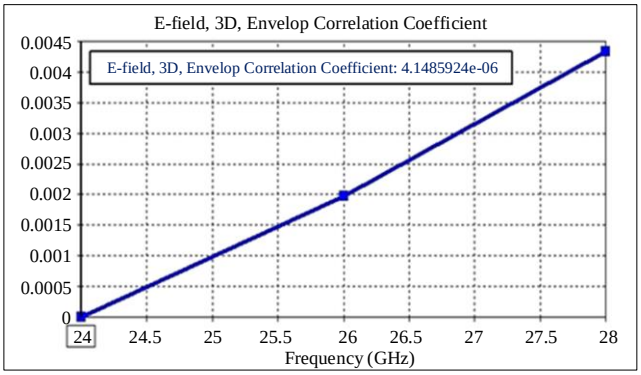

(a)

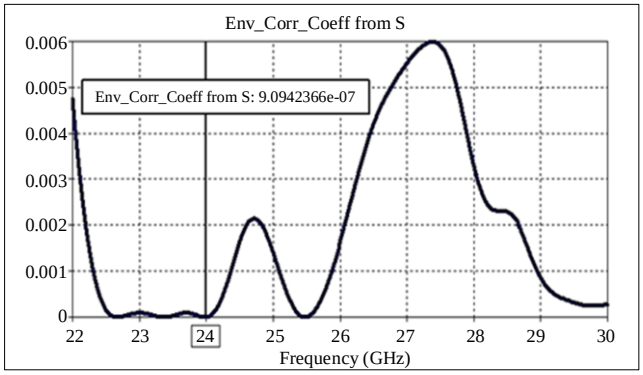

(b)

Fig. 17 ECC of 2x2 MIMO antenna with DSG evaluated using (a) Radiation pattern, and (b) S-parameter.

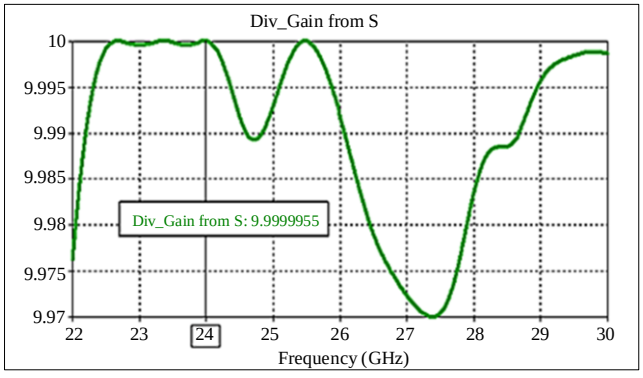

(a)

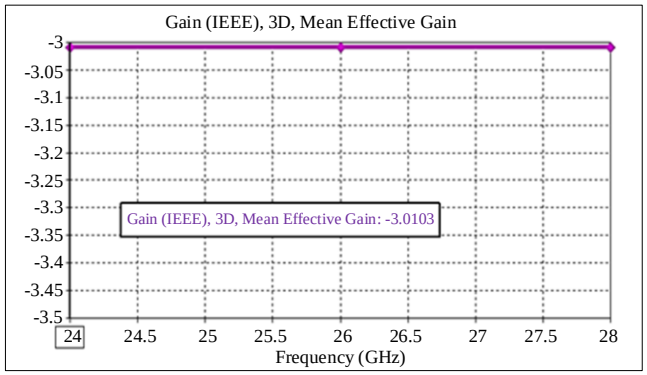

(b)

Fig. 18 2x2 MIMO antenna (a) Diversity-gain, and (b) MEG.

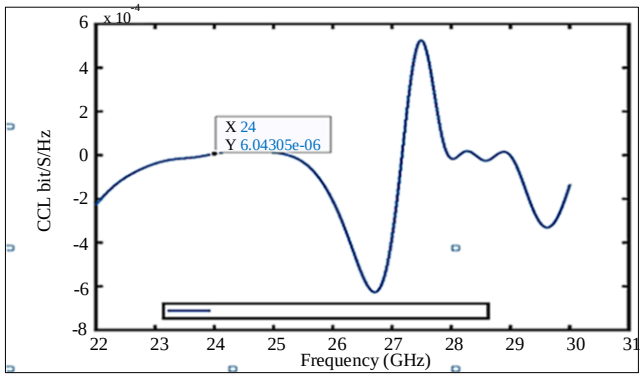

(a)

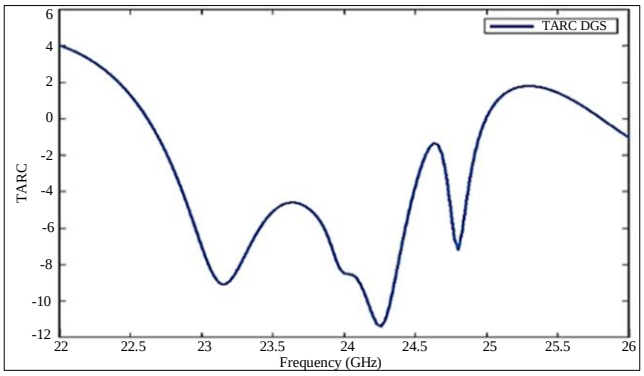

(b)

Fig. 19 The 2x2 MIMO with DGS (a) CCL, and (b) TARC.

4.7. Fabrication and Measurements

The fabricated 2x2 MIMO antenna structure with the slotted ground (Defective Ground Structure) is fabricated on Roger 5880 with the dimensions being 15mm x 15mm x 0.508mm. Figure 20(a) shows the top view, and (b) depicts the bottom view of the proposed system. The measurements of the S11 and S22 (reflection coefficients) and S12 and S21 (transmission coefficient) of the proposed antenna system are carried out through the Network Analyzer Agilent N5247A: A.09.90.02 as shown in Figure 21.

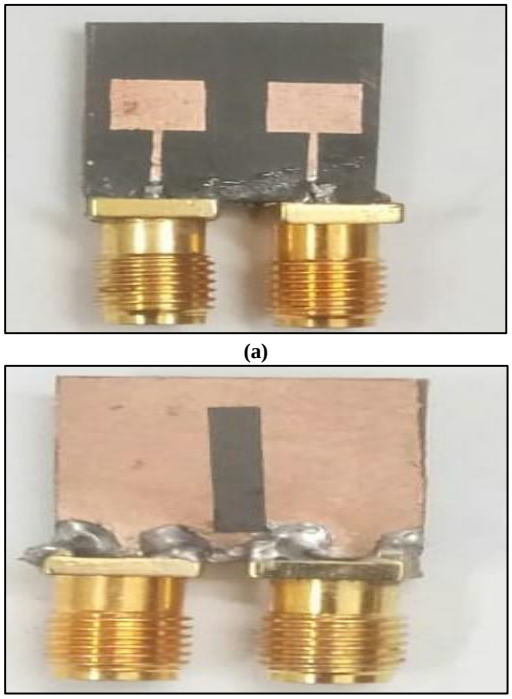

(a)

(b)

Fig. 20 Fabricated 2x2 MIMO antenna system with DSG (a) Top view, and (b) Bottom view.

Fig. 21 Measurement of S-parameter of fabricated 2x2 MIMO

The comparison of the simulation and measured results is shown in Figure 22(a) and (b). The obtained results are in good agreement with each other.

The S11 and S22 (reflection coefficient) of antenna-1 and antenna-2 indicate a 200MHz shift from the desired frequency, that is 24GHz. The proximity of the connections is the reason for this shift in position. The results indicate that the percentage difference between the simulation results and measured results is 0.8%.

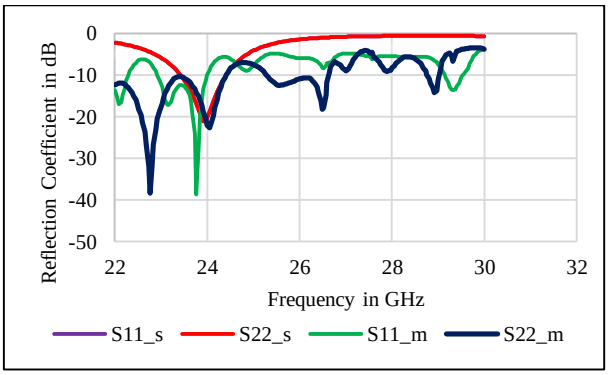

(a)

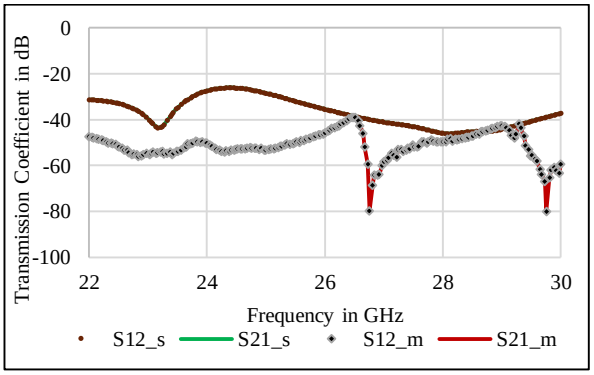

(b)

Fig. 22 The comparison graph of the measured and simulated system (a) Reflection coefficient, and (b) Transmission coefficient.

5. Performance Evaluation OSTBC Code with Designed 2x2 MIMO Loaded with and without DGS

The 2x2 quasi-static frequency-flat Rayleigh channel is employed to mimic a QPSK-modulated OSTBC. The system works at a frequency of 24 GHz. The estimated SNR range is 0 to 10 dB. The designed 2x2 multiple antenna are employed on the sending end (Tx) as well as the receive (Rx) sides.

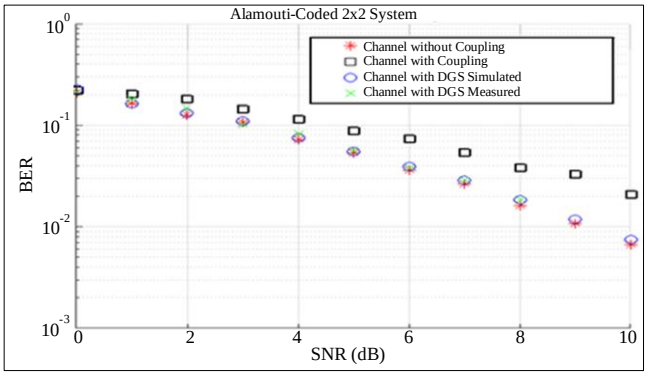

Fig. 23 Performance of multiple antenna transmission system with OSTBC and 2X2 multiple antenna placed at λ /4 apart

The microstrip antennas at the transmitter and receiver are λ/4 apart. The s-matrix of the simulated and fabricated

structure is considered to evaluate the coupling matrix for the transmitter and receiving antennas. The performance of multiple antenna systems with OSTBC, along with the 2x2 multiple-antenna system with and without defective ground structure, is studied. Figure 23 depicts the obtained findings.

The results obtained clearly indicate that closely placed antennas without DGS structure degrades the system performance. With the addition of an isolating structure between the antennas, the mutual coupling is reduced; thereby, the overall system performance is the same as a system with no coupling. The most important observation is that OSTBC performance can be improved with a closely placed antenna loaded with a DGS structure.

6. Conclusion

The work mainly intended to check the impact of mutual coupling of the closely spaced antenna with OSTBC in MIMO antenna system transmission. Initially, the 2X2 MRPA is designed to operate at 24GHz. The multiple antenna performance metrics are assessed for the 2X2 multiple-antenna system. The results have shown that 2x2 MIMO antenna evaluation metrics are better when the DGS acting as an isolating structure is introduced. The 2x2 multiple-antenna system loaded with DGS offers an ECC of 0.00004 when evaluated using a far-field pattern. Diversity and mean-effective-gain obtained are 9.999dB and -3dB.

The channel capacity loss is 0.000006 at 24GHz, and the TARC reported is below 0dB for the operating frequency range. Further, the analysis of the designed antenna with OSTBC code is performed. The results indicate that when antennas are not loaded with decoupling structure and are closely spaced, the system performances degrade, and the bit error rate is high, but when closely spaced antennas are loaded with the DGS, the performance is at par with the system offering zero or no coupling. Thus, OSTBC coding, along with the DGS-loaded 2x2 microstrip rectangular patch antenna, leads to better multiple antenna system transmission performance.

References

[1] Mahmood F. Mosleh, Raad H. Thaher, and Eman A., "SM High Data Rate Transmission over Multipath Channel Using MIMO with LDPC," *ZANCO Journal of Pure and Applied Sciences*, vol. 28, pp. 522-526, 2016. [Google Scholar]

[2] C.E. Shannon, "A Mathematical Theory of Communication, Part I, Part II," *The Bell System Technical Journal*, vol. 27, no. 3, pp. 623-656, 1948. [CrossRef] [Google Scholar] [Publisher Link]

[3] Carlos A.R. Martins, Mauro Luiz Brandão Jr., and Eduardo Brandani da Silva, "New Space-Time Block Codes from the Spectral Norm," *PLoS One*, vol. 14, no. 9, pp. 1-35, 2019. [CrossRef] [Google Scholar] [Publisher Link]

[4] Ahmad Baheej Al-Khalil, and Alyaa Al-Barrak, "Performance of BCH and RS Codes in MIMO System Using MPFEC Diversity Technique," *2018 International Conference on Advanced Science and Engineering*, pp. 122-127, 2018. [CrossRef] [Google Scholar] [Publisher Link]

[5] Nelson Costa, and Simon Haykin, *Multiple-Input, Multiple-Output Channel Models*, John Wiley & Sons, 2010. [Google Scholar]

[6] Emre Telatar, "Capacity of Multi-Antenna Gaussian Channels," *European Transactions on Telecommunications*, vol. 10, no. 6, pp. 585-595, 1999. [CrossRef] [Google Scholar] [Publisher Link]

[7] N. Al-Dhahir et al., "Space-Time Processing for Broadband Wireless Access," *IEEE Communications Magazine*, vol. 40, no. 9, pp. 136-142, 2002. [CrossRef] [Google Scholar] [Publisher Link]

[8] Hamid Jafarkhani, "Space-Time Coding: Theory and Practice," 2005. [Google Scholar] [Publisher Link]

[9] V. Tarokh, H. Jafarkhani, and A.R. Calderbank, "Spacetime Block Codes from Orthogonal Designs," *IEEE Transactions on Information Theory*, vol. 45, no. 5, pp. 1456-1467, 1999. [CrossRef] [Google Scholar] [Publisher Link]

[10] Branka Vucetic, and Jinhong Yuan, *Space-Time Coding*, John Wiley & Sons Ltd., 2003. [Google Scholar] [Publisher Link]

[11] V. Tarokh, N. Seshadri, and A.R. Calderbank, "Space-Time Codes for High Data Rate Wireless Communication: Performance Criterion and Code Construction," *IEEE Transactions on Information Theory*, vol. 44, no. 2, pp. 744-765, 1998. [CrossRef] [Google Scholar] [Publisher Link]

[12] S.M. Alamouti, "A Simple Transmit Diversity Technique for Wireless Communications," *IEEE Journal on Select Areas in Communications*, vol. 16, no. 8, pp. 1451-1458, 1998. [CrossRef] [Google Scholar] [Publisher Link]

[13] Zhi Ding, and Ye Li, *Blind Equalization and Identification*, Marcel Dekker, 2001. [CrossRef] [Google Scholar] [Publisher Link]

[14] C. Budianu, and L. Tong, "Channel Estimation for Space-Time Orthogonal Block Code," *IEEE Transactions on Signal Processing*, vol. 50, no. 10, pp. 2515-2528, 2002. [CrossRef] [Google Scholar] [Publisher Link]

[15] N. Ammar, and Z. Ding, "Channel Estimation under Space-Time Block Code Transmission," *Sensor Array and Multichannel Signal Processing Workshop Proceedings*, pp. 422-426, 2002. [CrossRef] [Google Scholar] [Publisher Link]

[16] A.L. Swindlehurst, and G. Leus, "Blind and Semi-Blind Equalization for Generalized Space-Time Block Codes," *IEEE Transactions on Signal Processing*, vol. 50, no. 10, pp. 2489-2498, 2002. [CrossRef] [Google Scholar] [Publisher Link]

[17] Petre Stoica, and Girish Ganesan, "Space-Time Block-Codes Trained, Blind and Semi-Blind Detection," *Proceedings of International Conference on Acoustics, Speech and Signal Processing*, vol. 13, no. 1, pp. 93-105, 2003. [CrossRef] [Google Scholar] [Publisher Link]

[18] Marvin K. Simon, and Mohamed-Slim Alouini, "Digital Communications over Fading Channels (M.K. Simon and M.S. Alouini; 2005) [Book Review]," *EEE Transactions on Information Theory*, vol. 54, no. 7, pp. 3369-3370, 2008. [CrossRef] [Google Scholar] [Publisher Link]

[19] Apinya Innok, Monthippa Uthansakul, and Peerapong Uthansakul, "The Enhancement of MIMO Capacity Using Angle Domain Processing Based on Measured Channels," *2009 Asia Pacific Microwave Conference*, pp. 2172-2175, 2009. [CrossRef] [Google Scholar] [Publisher Link]

[20] Kenichiro Kamohara, Hisato Iwai, and Hideichi Sasaoka, "Study of Channel Capacity Improvement by Open Loop Active Propagation Control," *2014 International Symposium on Antennas and Propagation Conference Proceedings*, pp. 113-114, 2014. [CrossRef] [Google Scholar] [Publisher Link]

[21] Bakar Rohani, and Hiroyuki Arai, "Channel Capacity Enhancement Using MIMO Antenna," *2018 IEEE International RF and Microwave Conference*, pp. 29-32, 2018. [CrossRef] [Google Scholar] [Publisher Link]

[22] Hedi Sakli et al., "Metamaterial-Based Antenna Performance Enhancement for MIMO System Applications," *IEEE Access*, vol. 9, pp. 38546-38556, 2021. [CrossRef] [Google Scholar] [Publisher Link]

[23] Priyanka Garg, and Priyanka Jain, "Isolation Improvement of MIMO Antenna Using a Novel Flower-Shaped Metamaterial Absorber at 5.5GHz WiMAX Band," *IEEE Transactions on Circuits and Systems II: Express Briefs*, vol. 67, no. 4, pp. 675-679, 2020. [CrossRef] [Google Scholar] [Publisher Link]

[24] Ziyang Wang et al., "A Meta-Surface Antenna Array Decoupling (MAAD) Method for Mutual Coupling Reduction in a MIMO Antenna System," *Scientific Reports*, vol. 8, pp. 3152-3159, 2018. [CrossRef] [Google Scholar] [Publisher Link]

[25] Cheng-Dai Xue et al., "MIMO Antenna Using Hybrid Electric and Magnetic Coupling for Isolation Enhancement," *IEEE Transactions on Antennas and Propagation*, vol. 65, no. 10, pp. 5162-5170, 2017. [CrossRef] [Google Scholar] [Publisher Link]

[26] Yang C. et al., "Quad-Band Antenna with High Isolation MIMO and Broadband SCS for Broadcasting and Telecommunication Services," *IEEE Antennas Wireless Propagation Letters*, vol. 9, pp. 584-587, 2010. [CrossRef] [Google Scholar] [Publisher Link]

[27] Ankan Bhattacharya, and Bappadittya Roy, "Investigations on an Extremely Compact MIMO Antenna with Enhanced Isolation and Bandwidth," *Microwave Optical Technology Letters*, vol. 62, no. 2, pp. 845-851, 2020. [CrossRef] [Google Scholar] [Publisher Link]

[28] Erik G. Larsson et al., "Massive MIMO for Next Generation Wireless Systems," *IEEE Communications Magazine*, vol. 52, no. 2, pp. 186-195, 2014. [CrossRef] [Google Scholar] [Publisher Link]

[29] Tianqi Peiet al., "A Low-Profile Decoupling Structure for Mutual Coupling Suppression in MIMO Patch Antenna," *IEEE Transactions Antennas and Propagation*, vol. 69, no. 10, pp. 6145-6153, 2021. [CrossRef] [Google Scholar] [Publisher Link]

[30] Rakesh N. Tiwari et al., "High Isolation 4-Port UWB MIMO Antenna with Novel Decoupling Structure for High Speed and 5G Communication," *Proceedings of the 2022 International Conference on Electromagnetics in Advanced Applications (ICEAA)*, pp. 336-339, 2022. [CrossRef] [Google Scholar] [Publisher Link]

[31] Asim Ghalib, and Mohammad S. Sharawi "TCM Analysis of Defected Ground Structures for MIMO Antenna Designs in Mobile Terminals," *IEEE Access*, vol. 5, pp. 19680-19692, 2017. [CrossRef] [Google Scholar] [Publisher Link]